Light Harvesting Semiconductor Core−Shell Nanocrystals: Ultrafast Charge Transport Dynamics of CdSe−ZnS Quantum Dots

Abhinandan Makhal,[†] Hongdan Yan,[‡] Peter Lemmens,[‡] and Samir Kumar Pal*[,†]

[†]Unit for Nano Science & Technology, Department of Chemical, Biological & Macromolecular Sciences, S. N. Bose National Centre for Basic Sciences, Block JD, Sector III, Salt Lake, Kolkata 700 098, India, and [‡]Institute for Condensed Matter Physics, TU Braunschweig, Mendelssohnstrasse 3, D-38106 Braunschweig, Germany

Received: August 31, 2009; Revised Manuscript Received: October 31, 2009

Capping or functionalization of semiconductor quantum dots (QDs) is unavoidable for their photostability in practical use including sensitizer and biological tagging agents. However, the efficiency of the electron/hole transport from the photoexcited QDs to the external environments across the capping shell is not well-understood. In this study we report on the femtosecond carrier dynamics of core−shell type CdSe−ZnS semiconductor QDs of various sizes. Steady-state spectroscopic studies followed by picosecond-resolved time correlated single photon counting (TCSPC) experiments on the complexation of the QDs with a well-known electron acceptor, benzoquinone (BQ), reveal that the complex is essentially static in nature. Femtosecond-resolved fluorescence upconversion experiments on the complex explore the dynamics of electron transport from core CdSe to BQ via ZnS shell. The dependence of the electron transport dynamics on the core size of the QDs has also been explored. We have also studied the dynamics of electron transport from the core CdSe of various sizes to another TiO_2 nanoparticle as an electron acceptor across the shell. Our studies support the relevance of core shell type semiconducting quantum dots in light harvesting devices.

Introduction

In recent years the interest in the injection of electrons or holes in systems showing quantum confinement is strongly growing. Particularly, harvesting solar light energy by using quantum dots (QDs) of different sizes with various band gap energies has received significant attention in the field of modern nanoscience.[1] Photoinduced exciton (electron−hole pair) generation and the control of the excited electron at the surface of the QDs are the key factors to decide on the use of the QDs in light harvesting applications including dye-sensitized solar cells,[2,3] light emitting diodes,[4] display devices,[5−7] biological tagging materials,[8−11] photocatalysis,[12] and photovoltaics.[13] A recent work[14] on size-dependent electron transfer (ET) from excited-state CdSe QDs into TiO_2 nanoparticles has demonstrated that the rate of electron transfer from a photoexcited bare CdSe (without a shell) to the TiO_2 monotonically increases with the decrease of the CdSe QDs diameter. This study clearly reveals the possibilities of implementing QDs as photosensitizers in dye-sensitized solar cells.[15,16] However, real applications of the QDs as reducing/electron transporting agents are expected to be limited by their insufficient long-term stability due to possible surface damage/oxidation. The alternative choices are the core−shell type QDs, wherein a protective shell is expected to prevent the core QDs from unwanted oxidative deterioration. Another important point to consider is the use of functionalized QDs as potential sensitizers in the light harvesting applications including QD-sensitized solar cells.[15,16] Although a number of devices rely on the light harvesting mechanism of functionalized QDs, a detailed understanding of the photoinduced charge transfer processes of the ligated (capped) QDs is lacking in the literature. This is the motive of the present work.

The specific question that needs to be addressed is the efficiency of charge transfer from a core of a QD to the outside environment via its augmenting shell (capping) compared to that in the case of a bare QD of similar size. As the photoinduced charge separation across the band gap of a QD (electron hole pair (EHP) generation) is the fundamental process in the physical migration of a charge particle (electron or hole) to the external environments, it is also important to investigate the nature of charge migration across the shell. In the present work using femtosecond-resolved fluorescence upconversion techniques, we have investigated charge transfer dynamics of CdSe−ZnS core−shell type semiconductor QDs of various core diameters as model systems. In order to study the nature of charge migration, we have used the well-known organic molecule benzoquinone (BQ) as an electron acceptor.[17] The details of the complexation of QDs with the BQ molecules have also been explored by using steady-state and picosecond-resolved time correlated single photon counting (TCSPC) spectroscopy. The femtosecond-resolved fluorescence transients are found to be distinct for the electron transfer processes in the QD−BQ complex compared to those of the QDs without BQ. The femtosecond-resolved electron transfer from the QDs with various sizes to the BQ molecules has been investigated. Finally, the characteristics of the charge transfer of the core−shell QDs with different sizes to another nanoparticle TiO_2, which is important component for the state of the art dye-sensitized solar cell,[15] has also been explored.

Materials and Methods

All quantum dots (QDs) are purchased from EVIDOTS, USA. Here we have studied three different sizes of QDs, namely, Adirondack green (Adi-green; crystal diameter 2.1 nm), Birch yellow (Bir-yellow; crystal diameter 3.2 nm), and Maple red-orange (Map-red; crystal diameter 5.2 nm). Toluene, TiO_2 (<50 nm) is obtained from Sigma Aldrich, and benzoquinone (BQ)

* Corresponding author. E-mail: skpal@bose.res.in. Fax: 91 33 2335 3477.
[†] S. N. Bose National Centre for Basic Sciences.
[‡] Institute for Condensed Matter Physics.

10.1021/jp908376b
Published on Web 12/14/2009

from Alfa Aesar. The concentration of QDs in the colloidal solutions of toluene and BQ are maintained in such a way that single photon excitation in our picosecond ($\sim 5 \times 10^{-6}$ M) and femtosecond ($\sim 70 \times 10^{-6}$ M) experiments is strictly assured. TiO_2−QD samples are prepared by vigorous stirring of the QDs and TiO_2 mixture (1:10) and then depositing a thin film on a quartz plate. In a comparative study we have also measured QD thin films on quartz plate. We kept the prepared thin films in a dark place for about 4 h for drying.

Steady-state absorption and emission are measured with a Shimadzu UV-2450 spectrophotometer and a Jobin Yvon Fluoromax-3 fluorimeter, respectively. Details of the picosecond-resolved spectroscopic data have been measured with a commercial time-correlated single-photon counting (TCSPC) setup from Edinburgh Instruments (instrument response function (IRF = 60 ps), excitation at 375 nm). The femtosecond-resolved fluorescence spectroscopy is measured using a femtosecond upconversion setup (FOG 100, CDP) in which the sample is excited at 375 nm (0.5 nJ per pulse), using the second harmonic of a mode-locked Ti-sapphire laser with an 80 MHz repetition rate (Tsunami, Spectra Physics), pumped by a 10 W Millennia (Spectra Physics). The fundamental beam is frequency doubled in a nonlinear crystal (1 mm BBO, $\theta = 25°$, $\phi = 90°$). The fluorescence emitted from the sample is up-converted in a nonlinear crystal (0.5 mm BBO, $\theta = 10°$, $\phi = 90°$) using a gate pulse of the fundamental beam. The up-converted light is dispersed in a double monochromator and detected using photon counting electronics. A cross-correlation function is obtained using Raman scattering from water displaying a full width at half-maximum (fwhm) of 165 fs. The femtosecond fluorescence decays are fitted using a Gaussian shape for the exciting pulse. A LEO 922 energy filtered transmission electron microscope (EFTEM) was used to characterize the internal structures of the samples and to analyze their elemental composition. For the TEM measurements, QD sample was dispersed in toluene, sonicated for 8 min, and then drop-coated over a carbon-coated grid (Cu mesh 200).

Results and Discussion

The steady-state absorption and emission spectra of the three quantum dot solutions in toluene are shown in Figure 1. The absorption spectra of the QDs show first excitonic peaks at 502, 556, and 591 nm for the Adi-green, Bir-yellow, and Map-red, respectively. In order to estimate the diameter of the core CdSe, we have followed an empirical formula given in the literature.[18] The estimated diameters of the QDs under study are 2.36, 3.17, and 4.21 nm. High resolution transmission electron microscopic (HRTEM) image of the Adi-green reported in the literature[19] reveals the diameter of the QD to be 4−4.5 nm. Considering the core−shell structure of the QD and thickness of ZnS monolayer to be 0.31 nm, it can be estimated that two to three monolayers of ZnS constitute the shell of the Adi-green QD. The estimated diameter of the Map-red (4.21 nm) is found to be somewhat different from that of the supplied value from the vendor (5.2 nm). Considering the value supplied by the vendor to be an overall crystallite diameter (core and shell together), the estimated monolayer number is 1−1.5. Thus, the shell thickness of the smaller QDs is apparently higher than that of the larger sized QDs. In order to resolve this issue, we have performed TEM studies on the QD as shown in Figure 2. The average diameter of the crystallite is found to be 6.5 nm, which reveals the number of ZnS monolayers to be three to four.

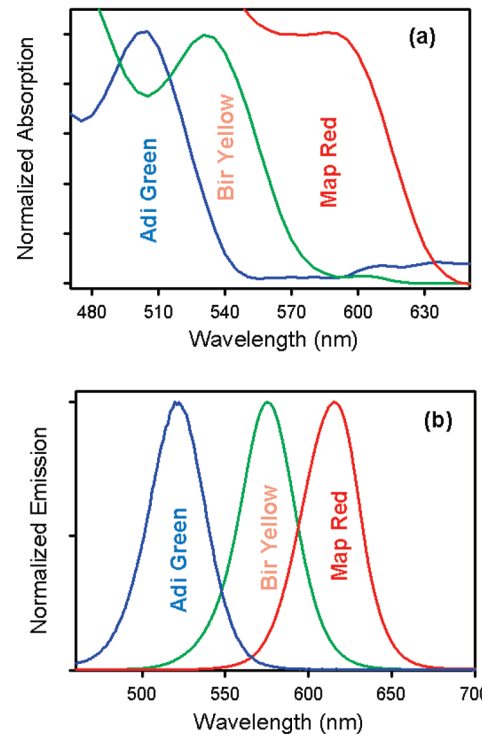

Figure 1. (a) The absorption spectra and (b) emission spectra of Adi-green (blue), Bir-yellow (green), Map-red (red) in toluene. We have used a 375 nm excitation for the emission measurements.

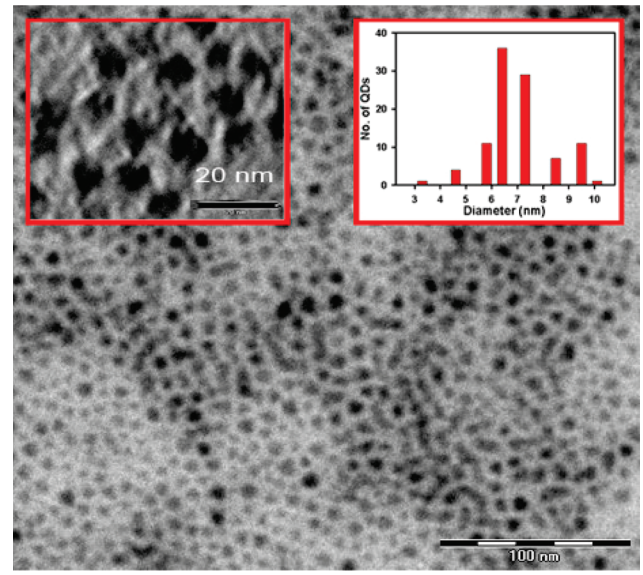

Figure 2. TEM image of Map-red qunatum dots. Inset of the figure (left side) shows a closer view of the QDs. Inset in the right side shows the size distribution of the QDs.

In order to study the electron transport across the ZnS shell of the QDs, we have used benzoquinone (BQ) as an electron-accepting agent.[17] Complexation of BQ with the QDs offers very efficient quenching of the QD emission as a consequence of the electron transfer reaction.[20] The complexation studies of BQ with smaller (Adi-green) and larger (Map-red) QDs are given in Figure 3. Insets of Figure 3a and 3b depict the change of fluorescence intensity (I) of the two QDs upon addition of the quencher BQ with respect to the intensity of the QD emission in the absence of BQ (I_0). The picosecond-resolved fluorescence transients of the QDs as shown in Figure 3a and 3b are fitted with triexponential function

$$\left(\sum_{i=1}^{3} A_i \exp\left(-\frac{t}{\tau_i}\right)\right)$$

where, A_is are weight percentages of the decay components with time constants of τ_i. The relative change in the overall excited-state lifetime

$$\left(\tau = \frac{\sum_{i=1}^{3} A_i\tau_i}{\sum_{i=1}^{3} A_i}\right)$$

with respect to that of the QDs without the quencher BQ (τ_0) is clearly evident from the figures. From Figure 3a and 3b it is also evident that steady-state emission quenching and shortening of excited-state lifetime of Adi-green is much faster compared to those of Map-red.

Our observation reveals that the plots (Supporting Information, Figure S1) of the relative steady-state emission intensity ($(I_0)/(I)$) and excited-state lifetime ($(\tau_0)/(\tau)$) vs BQ concentration ($[Q]$) in this study do not fit to the conventional Stern−Volmer (S−V) equation ($(I_0)/(I)$ or $(\tau_0)/(\tau) = 1 + K_{SV}[Q]$; K_{SV} is Stern−Volmer constant)[21] From Figure S1 in the Supporting Information it is also evident that the relative average lifetime ($(\tau_{AV0})/(\tau_{AV})$, where

$$\tau_{AV} = \frac{\sum_{i=1}^{3} A_i\tau_i^2}{\sum_{i=1}^{3} A_i\tau_i}$$

vs the BQ concentration plot does not follow a linear relationship. However, one can rationalize the quenching of the QDs in the presence of the quencher BQ as the decrease of emitting centers (N) relative to that in absence of BQ (N_0) from the following equation,[22,23]

$$N = N_0\left(\frac{I}{I_0} \times \frac{\tau_0}{\tau}\right) \quad (1)$$

Here we assumed N_0 to be 100. As shown in Figure 3c and 3d, the rate of change of the emitting centers of the smaller QDs is much faster than that of the larger QDs. As evidenced in the recent literature, the conclusion on the nature of the

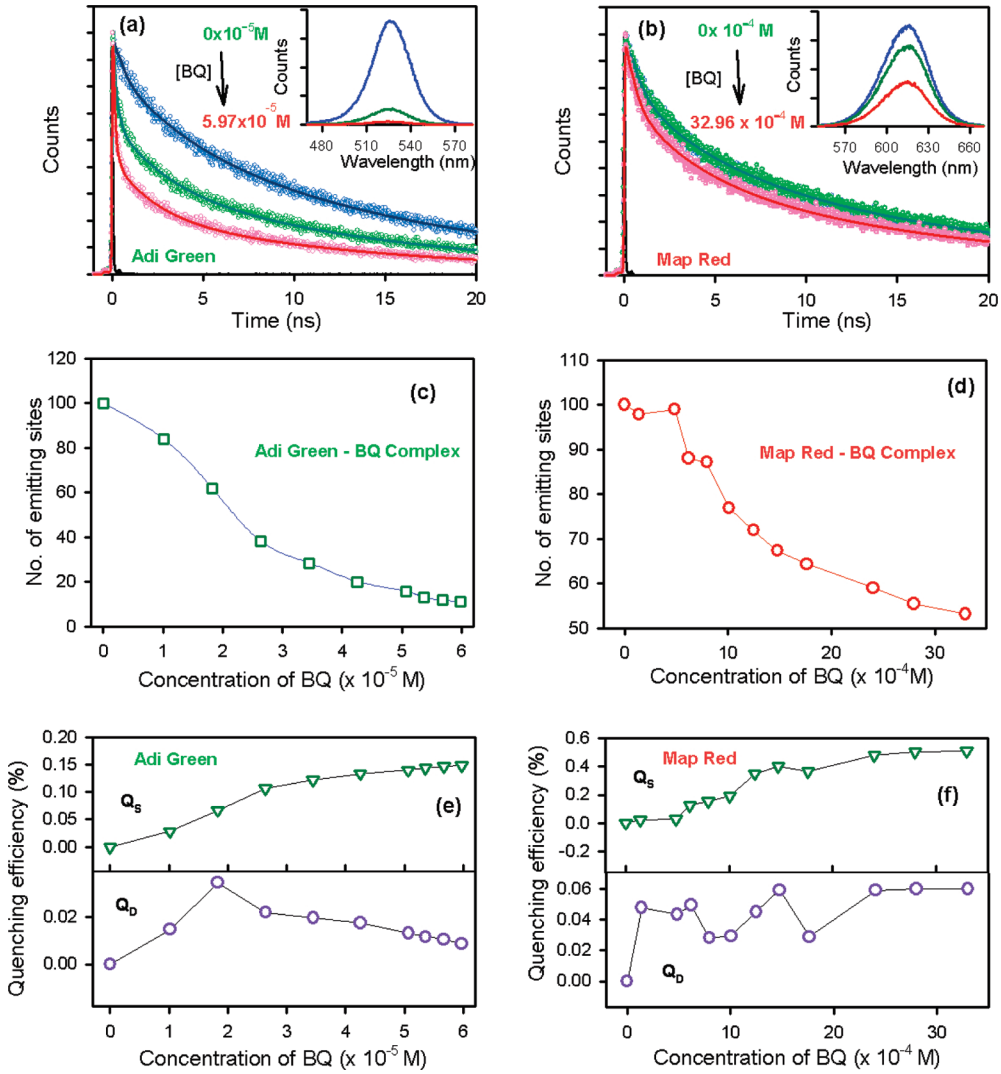

Figure 3. The picosecond-resolved fluorescence transients with different BQ concentrations of (a) Adi-green, (b) Map-red. Insets of a and b show steady-state emission spectrum of QDs with different BQ concentrations. None of the emitting sites of (c) Adi-green−BQ and (d) Map-red−BQ complexes as a function of BQ concentration are shown. Static (up) and dynamic (below) quenching efficiencies of (e) Adi-green and (f) Map-red as a function of BQ concentration are also shown.

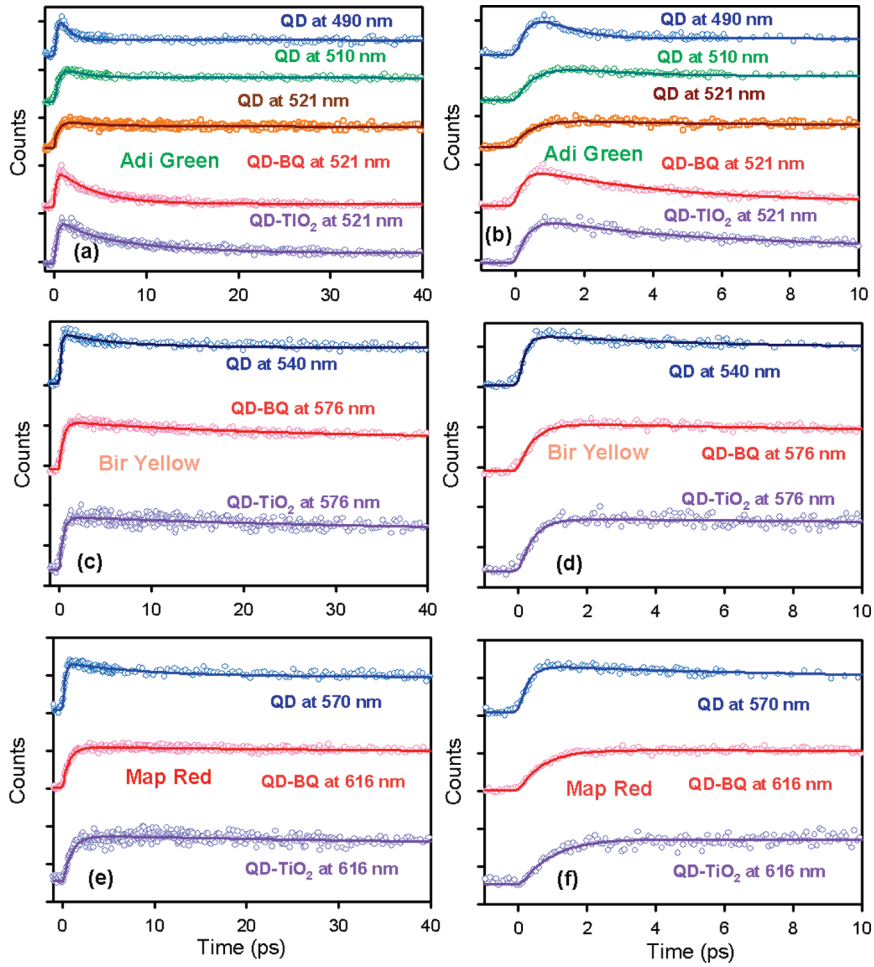

Figure 4. The femtosecond-resolved fluorescence transients of (a) Adi-green in toluene at 490, 510, and 521 nm wavelength, Adi-green-BQ at 521 nm and Adi-green−TiO_2 at 521 nm, (c) Bir-yellow at 540 nm, Bir-yellow-BQ at 576 nm, and Bir-yellow- TiO_2 at 576 nm, (e) Map-red in toluene at 570 nm, Map-red-BQ at 616 nm, and Map-red−TiO_2 at 616 nm. For a clear view, fast components are shown at right side of the respective figures.

quenching (static/dynamic) of QD fluorescence by organic molecules is not straightforward.[24] Here we also attempt to investigate the nature of QD quenching (static/dynamic) by BQ molecules. The relative change in intensities via static and dynamic processes with respect to those in the absence of the quencher are defined as static (Q_S) and dynamic (Q_D) quenching efficiencies. The static and dynamic quenching efficiencies Q_S and Q_D, respectively, can be expressed as,[24]

$$Q_S = \frac{\Delta I_S}{I_0} = \frac{\sum_{i=1}^{3}\left(A_{i0} - A_i \times \frac{N}{N_0}\right)\tau_{i0}}{\sum_{i=1}^{3} A_{i0}\tau_{i0}} \quad (2)$$

$$Q_D = \frac{\Delta I_D}{I_0} = \frac{(I_0 - I - \Delta I_S)}{I_0} = \frac{\sum_{i=1}^{3} A_i(\tau_{i0} - \tau_i) \times \frac{N}{N_0}}{\sum_{i=1}^{3} A_{i0}\tau_{i0}} \quad (3)$$

where ΔI_S and ΔI_D are the intensity change due to static and dynamic quenching, respectively, at different quencher concentrations. It is evident from Figure 3e and 3f that the emission quenching of both the QDs is taking place mainly because of static complexation of the QDs with the quencher BQ. Thus, in the studies of QD−BQ complexes in toluene, the diffusion of the BQ molecules is not expected to interfere in a significant manner. Our observations are consistent with a recent report on the complexation of hole-transporting organic molecules with core−shell type quantum dots.[24]

Femtosecond-resolved fluorescence transients of the QDs in various host environments are shown in Figure 4. Left and right columns reveal the transients in various experimental time windows. The transients of all the QDs in toluene show a general characteristic: an ultrafast rise, two relatively slower decays (picosecond (ps) range), and a long nanosecond (ns) decay component, which does not decay within our experimental time window. For Adi-green, the transient at the peak emission wavelength of 521 nm shows a rise component of 0.54 ps followed by decay components of 3.18 and 47.65 ps. An attempt to fit the transients with stretched exponential[14] failed because of the rise component in the transients. In the case of Bir-yellow at the peak emission wavelength of 576 nm, the rise component is found to be 0.49 ps and the decay components are 4.40 and 89.52 ps. The rise component of the fluorescence transient at the peak emission wavelength of 616 nm for the Map-red is measured to be 0.66 ps, and 4.5 and 229 ps are the decay time constants. The origin of the rise components in the fluorescence transients can be explained in terms of the excess energy of the excitation pulse (375 nm) compared to the band end energies of the QDs under study (Figure 1). In a recent study of the carrier dynamics in CdSe nanocrystals,[25] the excitation energy-dependent process has been correlated with the time for the

electron (or hole) to relax to the emitting band edge state. A discernible size dependence on the decay kinetics upon increasing the QD size from Adi-green to Map-red, both for shorter (3−5 ps) and longer (40−250 ps) time scales is evidenced from Figure 4. The radiative lifetime of the QDs is expected to decrease for smaller sizes because of increased e^-/h^+ wave function overlap and increased interaction with the surface. Klimov et al.[26] have measured 1P-to-1S relaxation using femtosecond transient absorption and found faster relaxation rates for smaller QDs due to quantum confinement in the QDs.

In order to investigate the dynamics of photoinduced electron transfer across the barrier shell, we have used a fast electron removal technique.[27] Infrared spectroscopic studies have shown that the carbonyl stretch vibration of the BQ is lowered in frequency as soon as the BQ adsorbs on the QD surface.[17] The adsorbed BQ then acts as an electron acceptor and removes the photoexcited electron from the conduction band in less time than the laser pulse duration (<120 fs).[20] Another study on electron transfer to BQ, naphthoquinone, and rhodamine B attached to CdSe and CdS nanoparticles reveals that the excited-state electron transfer process takes place from the thermalized excitons on the CdSe or CdS nanoparticles.[17,28] The study also concludes that the electron transfer is faster than the instrumental resolution of 200 fs, and its rate is limited by the thermalization process to the band gap exciton level. It is well-known for the organic dyes that the blue side of the PL spectrum indicates the pre-equilibrium state and the red end is indicative of the equilibrium state of the excited state.[29] Thus, the fluorescence transient in the blue end of a QD reveals the dynamics of the exciton prior to the relaxation to the emitting band edge state. On the other hand, the transient in the red end is indicative of the dynamics of the relaxed exciton in the band edge state. In order to investigate the thermalization dynamics in the core shell type CdSe−ZnS QDs, which is similar to the internal conversion dynamics in the QDs, we have studied fluorescence transients at higher energy (blue end of the emission spectrum) of QD emission. The fluorescence transients of Adi-green QD at 490 and 510 nm (emission peak at 520 nm) are shown in Figure 4a and 4b. The transient at 490 nm shows a rise component of 500 fs followed by a decay component of 700 fs along with a nanosecond component, which is persistent in our experimental time window. At 510 nm, the rise and decay components of 650 fs and 1.60 ps, respectively, become slower and have lost some of their contribution compared to those in the 490 nm fluorescence transient. Note that the time constants of the 510 nm transient are comparable to those of the fluorescent transient at a peak emission wavelength of 520 nm. Upon addition of BQ, the fluorescence transient at 520 nm shows a rise component of 500 fs followed by two decay components of 600 and 8.2 ps as shown in Figure 4a. The transient is similar to that of the QD without BQ at 490 nm with an additional time component of 8.2 ps.

In order to study the dynamics of photoexcited electrons of the QDs associated with host TiO_2 particles, which has importance in the realization of a QD-sensitized solar cell,[14,30] we have also investigated the fluorescence dynamics of Adi-green in TiO_2 nanoparticles as shown in Figure 4a. Numerical fitting of the fluorescence decay shows a rise component of 390 fs and two decay components of 1.57 and 8.41 ps. The electron transfer dynamics of the QD associated with TiO_2 nanoparticles resembles that in the QD−BQ complex. The similarity of the early dynamics of the QD−BQ and QD−TiO_2 complexes with that of QD without an electron acceptor at the blue end reveals that the thermalization of the excitons is essential prior to the

SCHEME 1: Schematic Diagram of Electron Transport of Adi-green and Map-red to BQ/TiO_2[a]

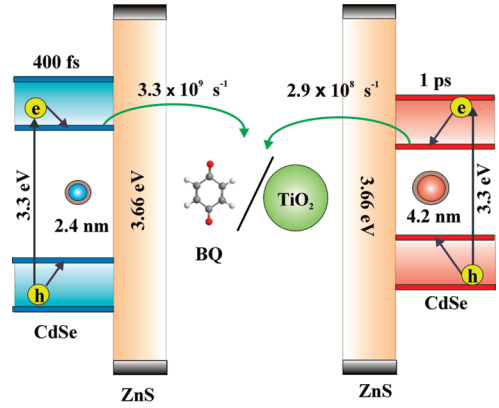

[a] After the thermalization of the excitons in QDs (400 fs and 1.0 ps in smaller and larger particles, respectively), the excited electron (3.3.eV excitation energy) can tunnel through the ZnS shell (3.66 eV band gap) to the attached electron acceptors with different rates, which depend on the size of the core of the QDs.

electron transfer process from the QD. The thermalization dynamics and the dynamics of electron transfer in relatively larger sized QDs are also evident from Figure 4c−f. The fluorescence transient of Bir-yellow (3.2 nm diameter) at its blue end of emission shows a rise of 180 fs followed by a decay component of 5.65 ps. In the case of QD−BQ complex at the peak emission wavelength, the rise component is 530 fs and decay components are 10.2 and 85.9 ps. The fluorescence transient of the QD with TiO_2 reveals a rise of 420 fs and decay components of 24.7 and 146.68 ps. The bigger sized QD Map-red shows relatively slower electron transfer dynamics as shown in Figure 4e and 4f. In the blue end of the emission at 570 nm, the QD shows a rise of 266 fs and decay component of 8.4 ps. In the QD−BQ complex at a peak emission wavelength of 616 nm, the rise component appears to be 720 fs which is followed by a decay component of 135.2 ps. The QD with a TiO_2 nanoparticle shows a rise of 950 fs with a decay component of 97.86 ps. From the above observation of the fluorescence transients of Bir-yellow and Map-red, it is also clear that thermalization of excitons, which is prominent in the dynamics at the blue ends of the emission of QDs without an electron acceptor, are essential prior to the electron transfer process to the attached electron acceptor BQ/TiO_2. An overall picture of the electron transfer process revealed from our studies can be summarized in Scheme 1. The femtosecond-resolved decay time constants as revealed from the numerical fitting from the fluorescence transients are summarized in Tables S1−4, Supporting Information.

In an attempt to compare the rate of electron transfer process of our QDs to TiO_2 nanoparticles with those reported in the literature,[14] we disregard the early rise component in the fluorescence transients and estimated the mean decay time constants of the QDs (τ_{QD}) and the QD−TiO_2 ($\tau_{QD\text{-}TiO2}$) complex. In order to estimate τ_{QD} we have studied thin films of QDs on quartz surfaces. The femtosecond decays of the QDs on the quartz plates are shown in Figure S2, and data are tabulated in Table S3 in the Supporting Information. The values of τ_{QD} and $\tau_{QD\text{-}TiO2}$ for Adi-green are 875.53 and 183.48 ps, respectively. For the Bir-yellow QDs, the values are 766.38 and 622.32 ps, respectively. In the case of Map-red, the time constants are 869.94 and 694.00 ps, respectively. Now the electron transfer rate k_{et} for different systems can be calculated as[14]

$$k_{et} = \frac{1}{\tau_{QD\text{-}BQ/TiO_2}} - \frac{1}{\tau_{QD}} \quad (4)$$

The rates (k_{et}) for the three QDs, Adi-green, Bir-yellow, and Map-red, are found to be 3.3×10^9 s^{-1}, 3.0×10^8 s^{-1}, and 2.9×10^8 s^{-1}, respectively. The details are tabulated in Table S5, Supporting Information. The smallest QD shows a faster electron transfer rate than that of the bigger QDs, due to the quantum confinement effect which increases the energy of its 1S electrons consequently facilitating the faster electron transfer rate.[28] The estimated rates are comparable to those reported in the literature for similar sized bare (without shell) CdSe QDs.[14] Our observation clearly indicates that the protective ZnS shell has minimal effect on the electron transfer dynamics from the QD core to the external environments and hence justifies the efficiency of the core−shell type QDs in electron transfer reactions. In a recent steady-state study of the efficiency of electron transport in core−barrier−shell semiconductor nanocrystals reveals a similar conclusion that the carrier electron can tunnel through the barrier ZnS shell.[16] In the case of QD−BQ complexes, the electron transfer rates are found to be similar to those in the QD−TiO_2 complexes. The similarity of the electron transfer dynamics of the QDs in BQ with those with TiO_2 rules out the possibility of interference of the dynamics of electron shuttling, which is the manifestation of electron−hole pair recombination via the BQ molecule.[27]

Conclusion

In summary, we have explored the photoinduced charge transport dynamics in core−shell type CdSe−ZnS semiconducting quantum dots with various core sizes. The study of femtosecond-resolved dynamics of photoinduced electron transport from the core to an electron-accepting organic molecule BQ reveals that thermalization of the excitons is a prior requirement for electron transport. The dynamical time constants associated with the electron transfer from the QD core to the outside electron acceptor via the shell are also found to depend on the size of the core. We have also explored the dynamical time scale associated to the electron transfer from core of the QDs to another TiO_2 nanoparticle through the shell. The characteristic rate is 3.3×10^9 s^{-1} for a 2.4 nm diameter particle and is 2.9×10^8 s^{-1} for a 4.2 nm diameter particle. These time scales are comparable to those reported for the bare CdSe quantum dots of similar sizes. Our studies justify the use of the most stable core−shell type semiconducting nanoparticles in light harvesting devices.

Acknowledgment. A.M. thanks CSIR, India, for a fellowship. We thank DST for a financial grant (SR/SO/BB-15/2007). Work was partially supported by the DFG, IGSM Braunschweig, and the Research Center "Contacs in Nanosystems, Project P1: Energy conversion in Molecular Nano Contacs".

Supporting Information Available: Time constants of the numerical fitting of the fluorescence transients are tabulated. The figures of the relative quenching of the QDs in the presence of various BQ concentrations are also shown. The fluorescence transients of the quantum dots on the quartz plates are shown. The rates of electron transfer across the ZnS shell of the QDs to TiO_2 particles are tabulated. The material is available free of charge via the Internet at http://pubs.acs.org.

References and Notes

(1) Robel, I.; Subramanian, V.; Kuno, M.; Kamat, P. V. *J. Am. Chem. Soc.* **2006**, *128*, 2385.
(2) O'Regan, B.; Gratzed, M. *Nature* **1991**, *353*, 737.
(3) Gratzel, M. *Nature* **2001**, *414*, 338.
(4) Alivisatos, A. P. *Science* **1996**, *271*, 933.
(5) Colvin, V. L.; Schlamp, M. C.; Alivisatos, A. P. *Nature* **1994**, *370*, 354.
(6) Tessler, N.; Medvedev, M. C.; Kazes, M.; Kan, S.; Banin, U. *Science* **2002**, *295*, 1506.
(7) Coe, S.; Woo, W. K.; Bawendi, G. M.; Bulovic, V. *Nature* **2002**, *420*, 800.
(8) Narayanan, S. S.; Sarkar, R.; Pal, S. K. *J. Phys. Chem. C* **2007**, *111*, 11539.
(9) Mattoussi, H.; Mauro, J. M.; Goodman, E.; Anderson, G. P.; C, S. V.; Mikulec, F. V.; Bawendi, M. G. *J. Am. Chem. Soc.* **2000**, *122*, 12142.
(10) Bruchez, M. J.; Moronne, M.; Gin, P.; Weiss, S.; Alivisatos, A. P. *Science* **1998**, *281*, 2013.
(11) Chan, W. C. W.; Nie, S. *Science* **1998**, *281*, 2016.
(12) Baruah, S.; S., S. S.; Ghosh, B.; Pal, S. K.; Raychaudhuri, A. K.; Dutta, J. *J. Appl. Phys.* **2009**, *105*, 074308.
(13) Huynh, W. U.; Dittmer, J. J.; Alivisatos, A. P. *Nature* **2002**, *295*, 2425.
(14) Robel, I.; Kuno, M.; Kamat, P. V. *J. Am. Chem. Soc.* **2007**, *129*, 4136.
(15) Kongkanand, A.; Tvrdy, K.; Takechi, K.; Kuno, M.; Kamat, P. V. *J. Am. Chem. Soc.* **2008**, *130*, 4007.
(16) Dias, E. A.; Sewall, S. L.; Kambhampati, P. *J. Phys. Chem. C* **2007**, *111*, 708.
(17) Burda, C.; Green, T. C.; Link, S.; El-Sayed, M. A. *J. Phys. Chem. B* **1999**, *103*, 1783.
(18) Yu, W. W.; Qu, L.; Guo, W.; Peng, X. *Chem. Mater.* **2003**, *15*, 2854.
(19) Narayanan, S. S.; Sinha, S. S.; Verma, P. K.; Pal, S. K. *Chem. Phys. Lett.* **2008**, *463*, 160.
(20) Lou, Y.; Chen, X.; Samia, A. C.; Burda, C. *J. Phys. Chem. B* **2003**, *107*, 12431.
(21) Lakowicz, J. R. *Principles of fluorescence spectroscopy*; Kluwer Academic/Plenum: New York, 1999.
(22) Carraway, E. R.; Demas, J. N.; DeGraff, B. A. *Anal. Chem.* **1991**, *63*, 332.
(23) Carraway, E. R.; Demas, J. N.; DeGraff, B. A.; Bacon, J. R. *Anal. Chem.* **1991**, *63*, 337.
(24) Zhang, Y.; Jing, P.; Zeng, Q.; Sun, Y.; Su, H.; Wang, Y. A.; Kong, X.; Zhao, J.; Zhang, H. *J. Phys. Chem. C* **2009**, *113*, 1886.
(25) Underwood, D. F.; Kippeny, T.; Rosenthal, S. J. *J. Phys. Chem. B* **2001**, *105*, 436.
(26) Klimov, V. I.; McBranch, D. W. *Phys. Rev. Lett.* **1998**, *80*, 4028.
(27) Burda, C.; Link, S.; Mohamed, M.; El-Sayed, M. *J. Phys. Chem. B* **2001**, *105*, 12286.
(28) Boulesbaa, A.; Issac, A.; Stockwell, D.; Huang, Z.; Huang, J.; Guo, J.; Lian, T. *J. Am. Chem. Soc.* **2007**, *129*, 15132.
(29) Pal, S. K.; Zewail, A. H. *Chem. Rev.* **2004**, *104*, 2099.
(30) Bang, J. H.; Kamat, P. V. *Acs. Nano.* **2009**, *3*, 1467.

JP908376B